

## Inhibition of Corrosion of Brass in 0.1 M H<sub>2</sub>SO<sub>4</sub> by Thioxopyrimidinone Derivatives

B.A.Abd-El-Nabey<sup>1\*</sup>, A.M.Abdel-Gaber<sup>1,2</sup>, E.Khamis<sup>1,3</sup>, Aly.I.A.Morgan<sup>1</sup> and N.M.Ali<sup>1</sup>

<sup>1</sup>Chemistry Department, Faculty of Science, Alexandria University, Ibrahimia , P.O.Box 426, Alexandria 21321 , Egypt.

<sup>2</sup>Chemistry Department, Faculty of Science, Beirut Arab University, Lebanon.

<sup>3</sup>City of Scientific Research & Technological Applications, New Borg El-Arab City, P.O. Box: 21934 Alexandria, Egypt

\*E-mail: [beshir\\_abdelnaby@yahoo.com](mailto:beshir_abdelnaby@yahoo.com)

Received: 13 June 2013 / Accepted: 9 July 2013 / Published: 20 August 2013

---

The inhibitive efficiency of 6-methyl-2-thioxopyrimidinone (MTP), 6-phenyl-2-thioxopyrimidin-4-one (PhTP) and 5-cyano-6-phenyl-2-thioxopyrimidin-4-one (CPhTP) for brass corrosion in 0.1 M H<sub>2</sub>SO<sub>4</sub> at 30°C were investigated by potentiodynamic polarization and electrochemical impedance spectroscopy (EIS) techniques. These compounds inhibit the corrosion of brass even at very low concentrations and the order of increasing the inhibition efficiency was correlated with the modification of the molecular structure of the inhibitors. The anodic polarization curves of brass in 0.1 M H<sub>2</sub>SO<sub>4</sub> in presence of higher concentrations of PhTP showed a passivity and limiting current behavior indicating the formation of [Cu(PhTP)]<sup>+</sup> sparingly soluble complex. Theoretical fitting of the kinetic-thermodynamic model of the adsorption of inhibitors at the metal surface are tested to clarify the nature of adsorption. Calculation of the activation parameters of the corrosion reaction of copper in absence and presence of the inhibitors indicated that the presence of the cyano group in CPhTP compound favors chemical adsorption of the inhibitor at the metal surface.

---

**Keywords:** Potentiodynamic polarization, EIS, Thioxopyrimidinones, Brass, H<sub>2</sub>SO<sub>4</sub>

### 1. INTRODUCTION

Copper and copper based alloys are of the most important materials used widely in different industries. Brass has been used in marine application and in heat exchange tubes, for example, in desalination, cooling water systems, power generation [1, 2] and petrochemical heat exchangers [3, 6]. Scale and corrosion products produced during the work of systems, have some negative effects on their heat-exchange performance, causing a decrease in heat efficiencies of the equipments. Thus acid washing is periodically carried out to de-scale and clean the systems. The degradation of basic metal in

pickling solutions is an undesirable reaction which should be diminished practically during the process. This can be achieved by the application of organic corrosion inhibitors. Nitrogen containing heterocyclic compounds may act as inhibitors for copper dissolution due to the chelating action of heterocyclic molecules and the formation of physical blocking barrier on the copper surface [7]. Benzotriazole is well known as an effective inhibitor of copper corrosion [8-10]. Schweinsberg et al. have done extensive research on the action of benzotriazole and its derivatives for copper corrosion in acidic solution [11-13]. Several researchers [14-19] studied the effect of some organic compounds such as tryptophan, isatin, DL-alanine and DL-cysteine, N-phenyl-1, 4-phenylenediamine, purine and adenine as copper corrosion inhibitor in acid solutions. Since, the S-atom has strong adsorption on copper, many heterocyclic compounds containing a mercapto groups have been used as copper corrosion inhibitors for different industrial applications. Zhang et al. [20] stated that introduction of mercapto group to heterocyclic compound can vary the disturbances and orbital energy configurations of electrons, thus enhancing the inhibitory effects on copper corrosion in acid solutions. Previous research has shown the inhibitory properties of 2-mercaptobenzothiazole, 2, 4-dimercaptopyrimidine, 2-amino-5-mercaptothiazole, 2-mercatothiazole, and 2-mercapto-1-methylimidazole [21-27]. The role of the mercapto group in relation to corrosion inhibition is still questionable until now. It has been suggested that corrosion inhibitor is chemisorbed on the copper surface through S- atom [18]. Other researcher proposed that interaction of the S-atom with the metal surface results in the formation of an insoluble protective complex [28].

The aim of the present work was to study the inhibition efficiencies of 6-methyl -2-thioxopyrimidin-4-ones (MTP), 6-phenyl-2-thioxopyrimidin-4-one (PhTP) and 5-cyano-6-phenyl-2-thioxopyrimidin-4-one (CPhTP) on the corrosion of brass in 0.1M H<sub>2</sub>SO<sub>4</sub>. Interest in these compounds relates to they contain N, O atoms,  $\pi$ -electrons and mercapto groups. Electrochemical methods such as potentiodynamic polarization and electrochemical impedance spectroscopy were used to determine their inhibition efficiencies and to investigate their inhibition mechanism.

## 2. EXPERIMENTAL

### 2.1 Electrochemical tests

Electrochemical impedance and polarization measurements were achieved using frequency response analyser (FRA)/potentiostat supplied from ACM instruments. The frequency range for electrochemical impedance spectroscopy (EIS) measurements was 0.1 to  $1 \times 10^{-4}$  Hz with applied potential signal amplitude of 10mV around the rest potential. The data were obtained in an electrochemical cell of three-electrode mode; platinum sheet and saturated calomel electrodes (SCE) were used as counter and reference electrodes. The material used for constructing the working electrodes were brass alloy ,red copper amd zinc.. The chemical composition of brass, red copper and zinc is given in table (1). The brass alloy ,red coper or zinc were encapsulated in epoxy resin in such a way that only one surface was left uncovered. The exposed area ( $0.785 \text{ cm}^2$  for brass ,  $0.2827 \text{ cm}^2$  for red copper and zinc ) was mechanically abraded with a series of emery papers of variable grades,

starting with a coarse one and proceeding in steps to the finest (600) grade. The samples were then washed thoroughly with double distilled water, followed with A. R. ethanol and finally with distilled water, just before insertion in the cell. Each experiment was carried out with newly polished electrode. Before polarization and EIS measurements, the working electrode was introduced into the test solution and left for 20 min to attain the open circuit potential. Polarization curve measurements were obtained at a scan rate of 20mV/min starting from cathodic potential ( $E_{corr}$ -250mV) going to anodic direction. All the measurements were done at  $30.0 \pm 0.1^\circ\text{C}$  in solutions open to the atmosphere under unstirred conditions.

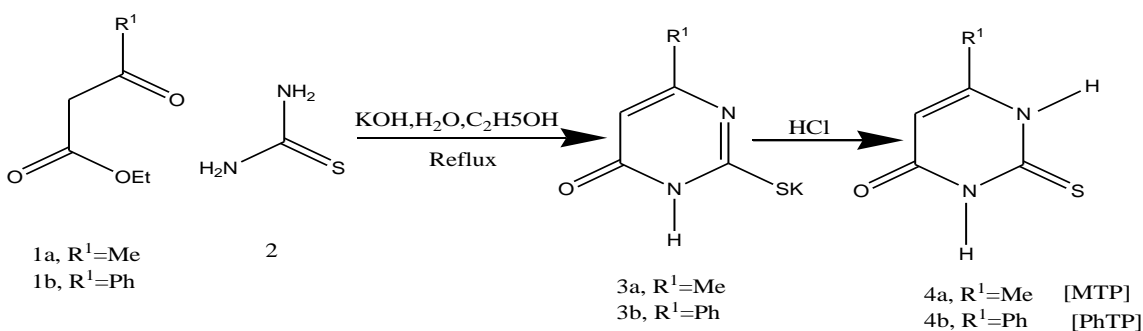
**Table 1.** Chemical composition of working electrodes specimens (Wt%)

brass alloy	Ca	Sn	Mo	Fe	Zn	Cu
	0.9	0.2	0.1	0.8	31.4	59.3
Red copper	Cu	Ca				
	99.5	0.5				
Zinc	Ca	Pb	Zn			
	0.4	1.0	98.5			

## 2.2 Preparation of the Inhibitors

### i) Synthesis of 6-methyl or phenyl-2-thioxopyrimidin-4-one(4a-b) [MTP,PhTP]:

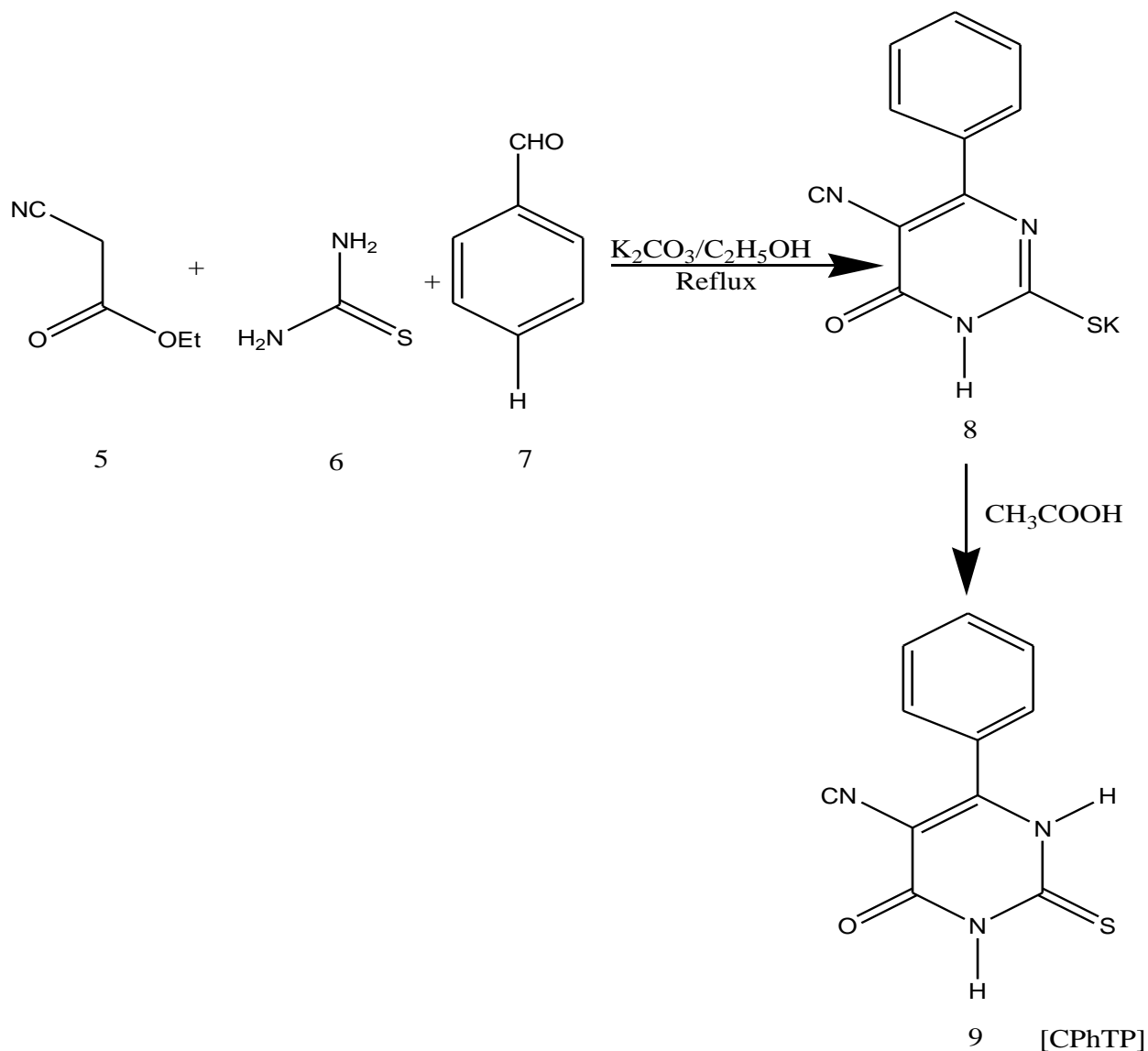
A mixture of ethyl acetoacetate (1a, 0.01 mol), or ethyl benzoylacetate(1b, 0.01 mol) and thiourea (2, 0.01 mol) in ethanol(20 mL) was treated with a solution of potassium hydroxide (0.01 mol) in water(5mL). The mixture was heated at reflux for 2 hrs, cooled and acidified with concentrated hydrochloric acid during stirring. The separated product (4a-b) was collected by filtration, washed with water and recrystallize from ethanol as a pale yellow crystal. The product (4a-b) was identified by TLC, m.p and spectral data.



### ii) Synthesis of 5-cyano-6-phenyl-2-thioxopyrimidin-4-one (9)[CPhTP]:

A mixture of ethyl cyanoacetate (5, 0.01 mol), thiourea (6, 0.01 mol) and aromatic aldehyde [benzaldehyde (7), 0.01 mol in ethanol(20 mL)] containing potassium carbonate (0.01 mol) was heated at reflux for 5 hrs. The precipitated potassium salt (8a-b) was collected by filtration and washed with

ethanol and dissolved in hot water (80°C) by stirring until a clear solution is obtained. After cooling, the solution was acidified with acetic acid and the formed product (9a-b) was collected by filtration and recrystallize from acetic acid as yellow crystals. The desired product (9) was identified by TLC, m.p. and spectral data.



### 2.3. Preparation of solutions

The aqueous solution used was 0.1M  $H_2SO_4$  prepared from 1M  $H_2SO_4$  diluted from analytical grade (Aldrich chemicals) concentrated acid 98% M  $H_2SO_4$  with doubly distilled water and was used without further purification. Stock solutions of the thiopyrimidinone derivatives were prepared to the appropriate concentrations ( $1 \times 10^{-2}M$  and  $1 \times 10^{-3}M$ ) and dissolved in DMF (dimethyl foramide).

The aqueous solution used for corrosion measurement is prepared by taking 5ml from 1M  $H_2SO_4$  to 50 ml measuring flask then add different volumes from the prepared stock solutions of thiopyrimidinone derivatives to prepare different concentrations then add the required volume of dimethyl foramide (DMF) to obtain 10% DMF in the examined solutions and then complete the volume to 50 ml with distilled water

### 3. RESULTS AND DISCUSSION

The aim of this work is to investigate the inhibitive action of 6-methyl-2-thioxopyrimidin-4-one (MTP), 6-phenyl-2-thioxopyrimidin-4-one (PhTP) and 5-cyano-6-phenyl-2-thioxopyrimidin-4-one (CPhTP) on the corrosion of brass in 0.1 M H<sub>2</sub>SO<sub>4</sub> at 30<sup>0</sup>C using potentiodynamic polarization and electrochemical impedance spectroscopy techniques.

#### 3.1. Polarization curves measurements results

Figure 1 shows the potentiodynamic polarization curves of brass in 0.1M H<sub>2</sub>SO<sub>4</sub> in absence and presence of different concentrations of MTP. The cathodic parts of the polarization curves show limiting current corresponds to the oxygen reduction reaction that is slightly affected by the addition of MTP. This indicates that the cathodic process is controlled by diffusion of oxygen gas from the bulk solution to the metal surface.

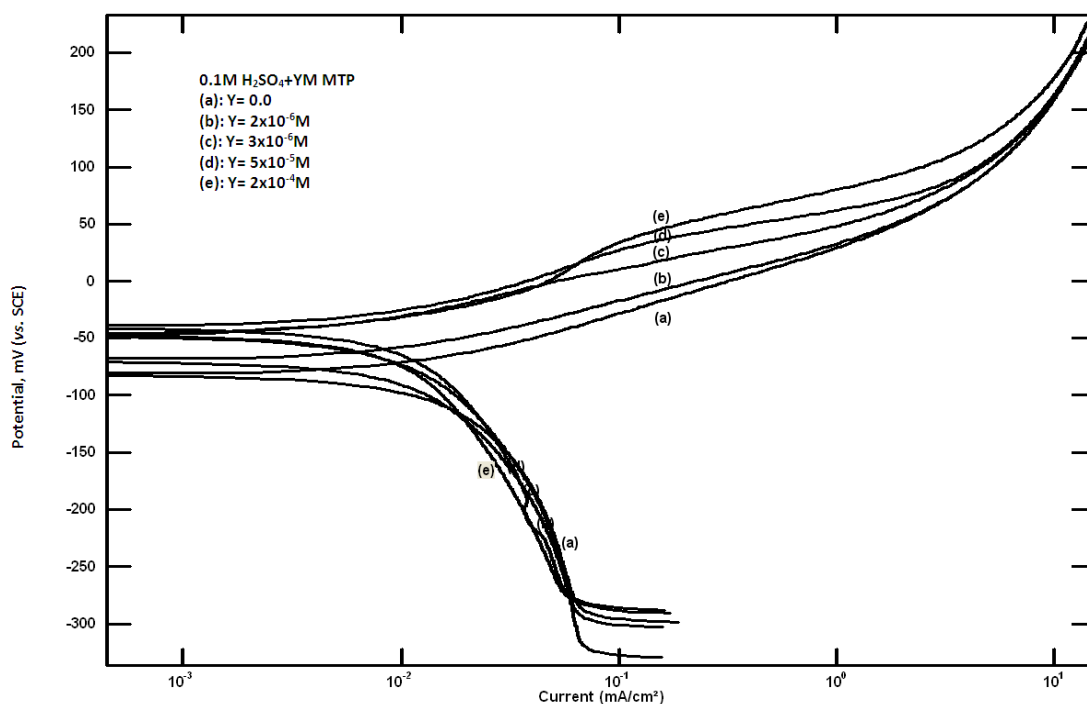


**Figure 1.** Potentiodynamic polarization curves of brass in 0.1M H<sub>2</sub>SO<sub>4</sub> in absence and presence of different concentrations of MTP.

This behavior is well known since copper can hardly be corroded in the deoxygenated dilute sulfuric acid [29], as copper cannot displace hydrogen from acid solutions according to theories of chemical thermodynamics. However, in aerated sulfuric acid, dissolved oxygen is reduced on copper surface and this will enable some corrosion to take place [30]. Cathodic reduction of oxygen can be expressed either by two consecutive 2e<sup>-</sup> steps involving a reduction to hydrogen peroxide first followed by a further reduction to water or by a direct 4e<sup>-</sup> transfer step [31] as shown by equation.



Addition of MTP slightly affects the values of corrosion potential and shift the anodic polarization curves to lower current density indicating that this compound act as anodic type inhibitor. The anodic part of the polarization curves for brass in presence of high MTP concentration shows (i) Tafel behavior indicating that the oxidation process is mainly controlled by charge transfer and (ii) inflection in the curve at about +0.02V(Vs SCE) which probably corresponds to the oxidation of Cu(I) to Cu(II). Since it was reported that the anodic dissolution of copper in acidic solutions can be illustrated by the following two consecutive steps [32]:

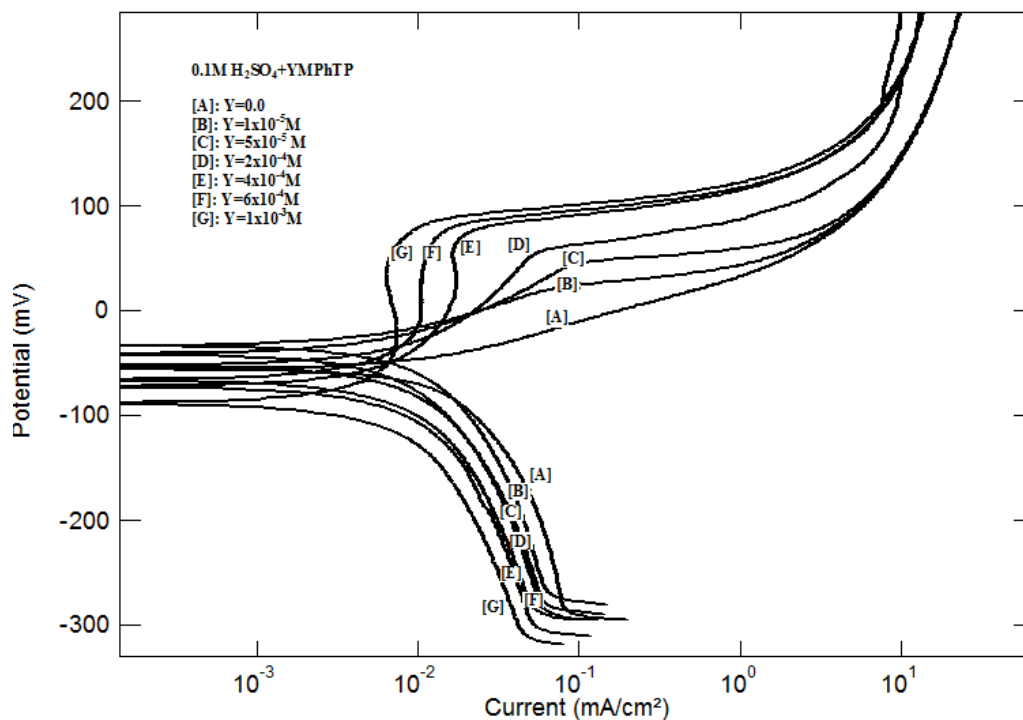
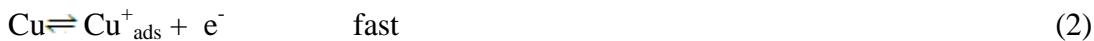


**Figure 2.** Potentiodynamic polarization curves of brass in 0.1M H<sub>2</sub>SO<sub>4</sub> in absence and presence of different concentrations of PhTP

Figure 2 shows the potentiodynamic polarization curves of brass in 0.1M H<sub>2</sub>SO<sub>4</sub> in absence and presence of different concentrations of PhTP. This compound affects both the cathodic and the anodic polarization curves and shift the corrosion potential to more anodic values indicating that it acts as mixed type inhibitor. The cathodic part of the polarization curves shows a limiting current behavior as in the case of MPT. In presence of small concentrations of PhTP, the anodic curves give a Tafel behavior and polarized to anodic potentials. However, in presence of high concentrations of PhTP the anodic polarization curves show a passivity and limiting current behavior which can be discussed on the basis of the formation of a sparingly soluble complex of Cu(I) or Zn(II).

The electrochemical potentiodynamic polarization parameters, i.e. corrosion potential ( $E_{\text{corr}}$ ), cathodic and anodic Tafel line slopes ( $\beta_c$ ,  $\beta_a$ ), and the corrosion current density ( $i_{\text{corr}}$ ), obtained from the

intersection of the anodic and cathodic Tafel lines with the corresponding corrosion potential are given in Table 2. It has been shown that in the Tafel extrapolation method, use of both the anodic and cathodic Tafel regions is undoubtedly preferred over the use of only one Tafel region [33]. The corrosion rate can also be determined by Tafel extrapolation of either the cathodic or anodic polarization curve alone. If only one polarization curve alone is used, it is generally the cathodic curve which usually produces a longer and better defined Tafel region. Anodic polarization may sometimes produce concentration effects, due to passivation and dissolution, as well as roughening of the surface which can lead to deviations from Tafel behavior [34].

The data indicate that as the inhibitor concentration increases, the corrosion current density decreases. The percentage of inhibition efficiency (%P) was calculated from the polarization curves measurements using the relation:

$$\%P = [((i_{\text{corr}})_0 - i_{\text{corr}}) / (i_{\text{corr}})_0] \times 100$$

where  $(i_{\text{corr}})_0$  and  $i_{\text{corr}}$  are the corrosion current densities, in the absence and the presence of inhibitor.

In order to explain the type of sparingly soluble complex formed on brass surface which may be attributed to the formation of a sparingly soluble complex of Cu(I) or Zn(II). It is worth to investigate the potentiodynamic polarization curves of zinc and red copper in 0.1M H<sub>2</sub>SO<sub>4</sub> in absence and presence of different concentrations of PhTP. Figure 3 shows the polarization curves of zinc in 0.1M H<sub>2</sub>SO<sub>4</sub> in absence and presence of different concentrations of PhTP.

**Table 2.** Electrochemical polarization parameters of brass in 0.1M H<sub>2</sub>SO<sub>4</sub> in absence and presence of different concentrations of MTP and PhTP

Solution	[inhibitor], mol. L <sup>-1</sup>	E <sub>corr</sub> , (mV vs. SCE)	β <sub>a</sub>	-β <sub>c</sub>	i <sub>corr</sub> , mA/cm <sup>2</sup>	%P
			(mV.decade <sup>-1</sup> )			
<b>0.1M H<sub>2</sub>SO<sub>4</sub></b>	0.00	-58	57	788	0.03127	0
<b>0.1M H<sub>2</sub>SO<sub>4</sub> +MTP</b>	2x10 <sup>-6</sup>	-21	38	538	0.02275	27.2
	3 x10 <sup>-6</sup>	-19	38	542	0.01922	38.5
	2 x10 <sup>-5</sup>	-28	64	478	0.01776	43.2
	5 x10 <sup>-5</sup>	-18	56	467	0.01658	46.9
	1 x10 <sup>-4</sup>	-39	82	426	0.01579	49.5
	2 x10 <sup>-4</sup>	-50	101	387	0.01480	52.6
<b>0.1M H<sub>2</sub>SO<sub>4</sub> +PhTP</b>	6x10 <sup>-6</sup>	8	16	492	0.01865	40.3
	1 x10 <sup>-5</sup>	10	18	481	0.01663	46.8
	2 x10 <sup>-5</sup>	19	18	480	0.01581	49.4
	5 x10 <sup>-5</sup>	-18	78	426	0.01453	53.5
	2x10 <sup>-4</sup>	-36	155	382	0.01397	55.3
	4 x10 <sup>-4</sup>	-35	292	407	0.01154	63.0
	6 x10 <sup>-4</sup>	-16	540	385	0.01048	66.5
8 x10 <sup>-4</sup>	-13	582	326	0.007429	76.2	

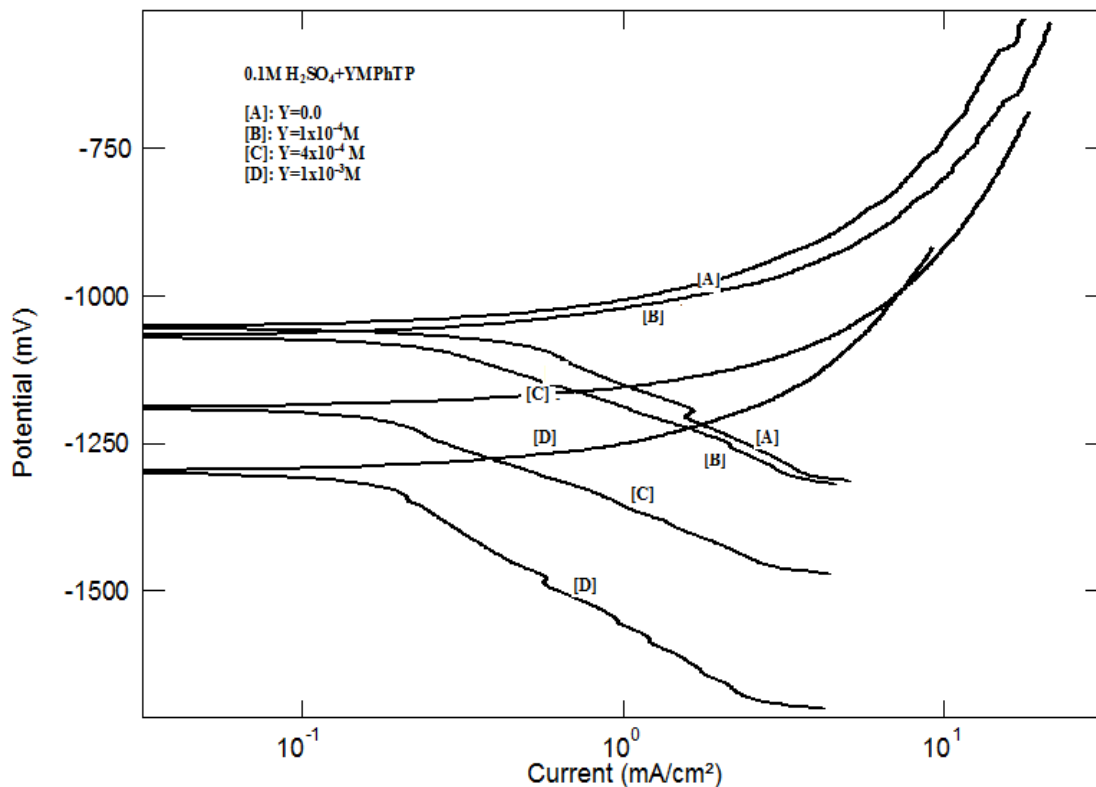


**Figure 3.** Potentiodynamic polarization curves of Zinc in 0.1M H<sub>2</sub>SO<sub>4</sub> in absence and presence of different concentrations of PhTP

The figure clarifies typical Tafel behavior that is greatly differing from that obtained for brass. This is because, for the active zinc metal in acid solutions, when dissolved in presence of oxygen, both hydrogen evolution and oxygen reduction reactions will be possible. However, in view of the fact that, the saturated solubility of oxygen in pure water at 25°C is only about 10<sup>-3</sup> mol dm<sup>-3</sup> [35] and decreases slightly with increasing the concentration of dissolved salts. In addition, the concentration of H<sub>3</sub>O<sup>+</sup> in acid solutions, at pH ≈ 0, is high, and since this ion has a high rate of diffusion, consequently, the contribution of the hydrogen evolution reaction at the cathodic process will overcome the oxygen reduction reaction. Therefore, the corrosion of zinc in acid solution proceeds via two partial reactions [36]. The partial cathodic reaction involves evolution of hydrogen gas.



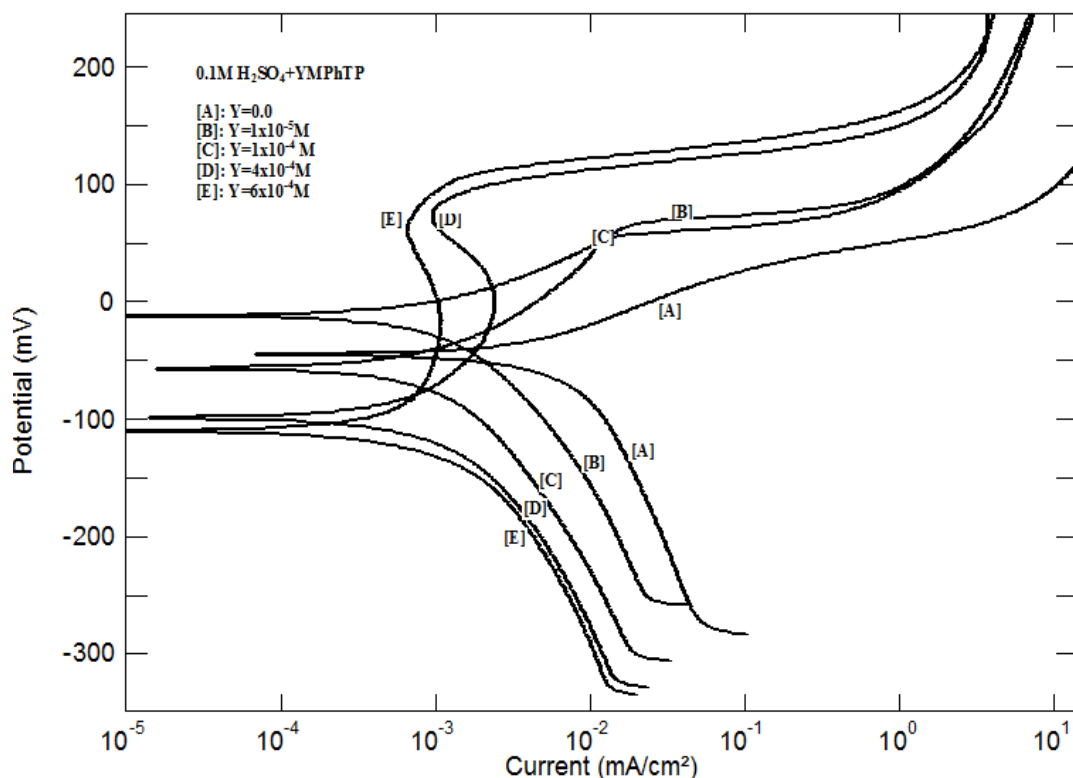
The partial anodic reaction involves the oxidation of Zn and formation of soluble Zn<sup>2+</sup>



Figure 4 shows the polarization curves of red copper in 0.1M H<sub>2</sub>SO<sub>4</sub> in absence and presence of different concentrations of PhTP.. In case of red copper, the cathodic polarization curves show limiting current and the anodic curves in absence and presence of small concentrations of inhibitor there is continuous corrosion while in presence of higher concentrations of inhibitor a passive film formed. It is clear that red copper gives the same behavior as brass and there is passivity and limiting current behavior obtained. These observations indicate that the suggested complex formed is mainly



$\text{Cu}[\text{PhTP}]^+$ . Diffusion of this complex from the surface of brass to the bulk solution is probably the slow step of the oxidation of copper.



**Figure 4.** Potentiodynamic polarization curves of red copper in 0.1M  $\text{H}_2\text{SO}_4$  in absence and presence of different concentrations of PhTP.

Figure 5 shows the potentiodynamic polarization curves of brass in 0.1M  $\text{H}_2\text{SO}_4$  in the absence and presence of different concentrations of CPhTP. The cathodic part of the polarization curves show limiting current slightly affected by the addition of CPhTP indicating that the cathodic process is controlled by diffusion of oxygen from the bulk solution to the metal surface. Addition of CPhTP shift the corrosion potential to more anodic values and shift the anodic part of the polarization curves to more noble value indicating that it acts as mixed type inhibitor. Furthermore, the anodic part of the polarization curve in presence of different concentrations of CPhTP show (i) A Tafel behavior indicating that the oxidation of copper is mainly controlled by charge transfer (ii) An inflection in the curve which probably corresponds to the oxidation of Cu(I) to Cu(II). This behavior is similar to that obtained in case of MTP. The values of the electrochemical polarization parameters,  $E_{\text{corr}}$ ,  $i_{\text{corr}}$ ,  $\beta_a$  and  $\beta_c$  at different concentrations of CPhTP are given in Table 3. The data revealed that as the inhibitor concentration increases, the corrosion current density decreases but slightly affects the values of corrosion potential ( $E_{\text{corr}}$ ). Maximum inhibition of 96.1% is obtained on adding  $4 \times 10^{-4}$  M CPhTP. Higher values of  $\beta_c$  have been obtain due to the presence of limiting current and the cathodic process is controlled by diffusion.

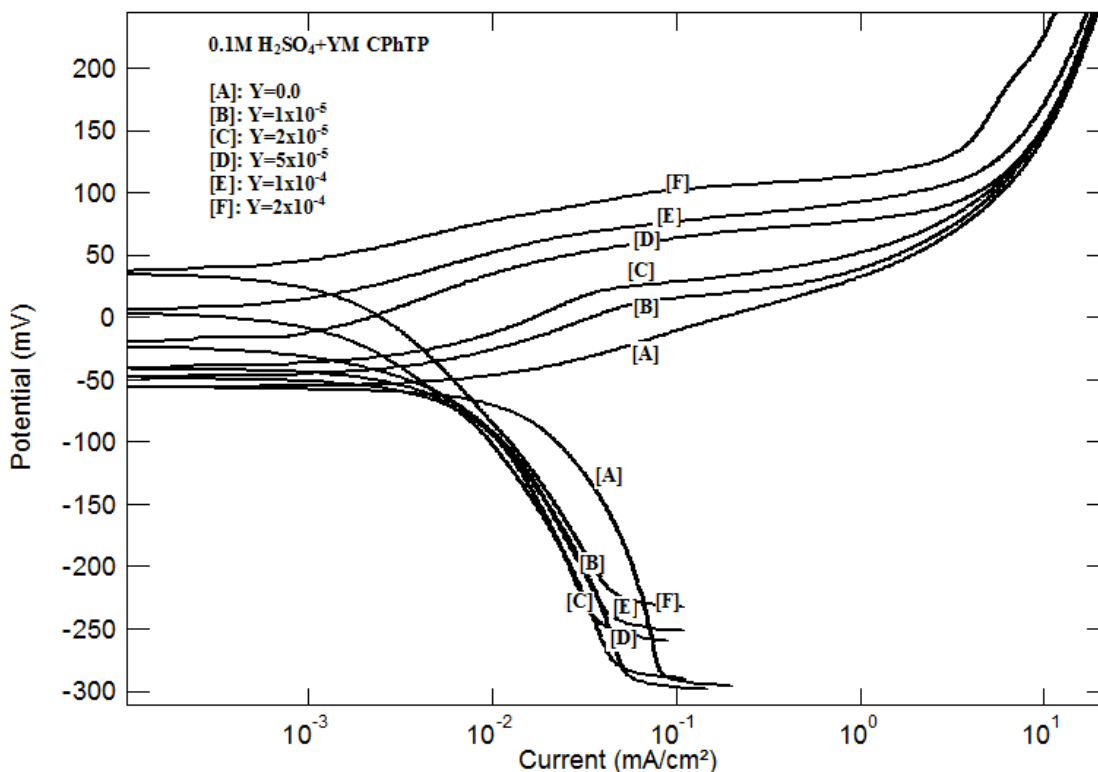


**Figure 5.** Potentiodynamic polarization curves of brass in 0.1M H<sub>2</sub>SO<sub>4</sub> in absence and presence of different concentrations of CPhTP.

**Table 3.** Electrochemical polarization parameters of brass in 0.1M H<sub>2</sub>SO<sub>4</sub> in absence and presence of different concentrations of CPhTP.

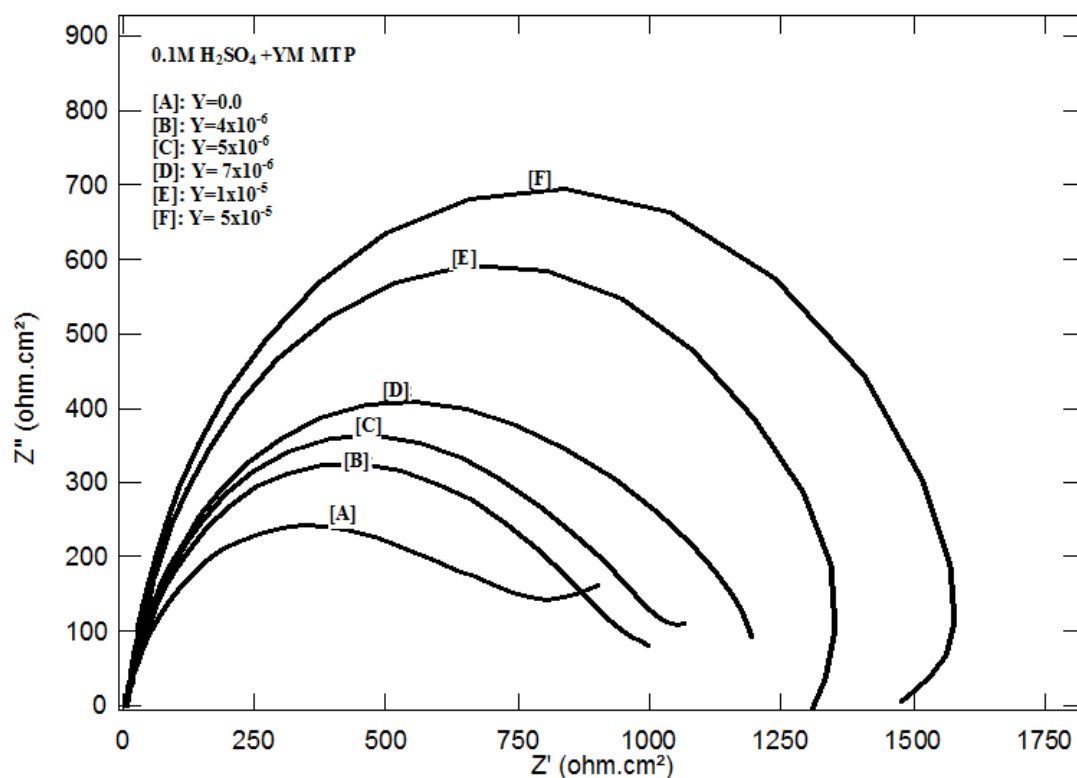
Solution	[inhibitor], mol. L <sup>-1</sup>	E <sub>corr</sub> , (mV vs. SCE)	β <sub>a</sub> -β <sub>c</sub>		i <sub>corr</sub> , mA/cm <sup>2</sup>	%P
			(mV.decade <sup>-1</sup> )			
<b>0.1M H<sub>2</sub>SO<sub>4</sub></b>	0.00	-58.0	57	788	0.03127	0
<b>0.1M H<sub>2</sub>SO<sub>4</sub> + CPhTP</b>	6x10 <sup>-6</sup>	-10.4	29	350	0.01543	50.7
	7 x10 <sup>-6</sup>	-2.4	19	416	0.01430	54.3
	8 x10 <sup>-6</sup>	-6.7	25	340	0.01333	57.4
	1 x10 <sup>-5</sup>	-19.2	42	414	0.01168	62.6
	1.5 x10 <sup>-5</sup>	0.39	20	419	0.00897	71.3
	2 x10 <sup>-5</sup>	-12.1	49	354	0.00813	74.0
	5 x10 <sup>-5</sup>	22.5	41	319	0.00520	83.4
	1 x10 <sup>-4</sup>	40.9	32	287	0.00439	85.9
	2 x10 <sup>-4</sup>	59.4	29	233	0.00274	91.2
4x10 <sup>-4</sup>	53.8	25	201	0.00121	96.1	

It is clear that this cyano compound is more efficient in the inhibition of the corrosion of yellow copper in 0.1 M H<sub>2</sub>SO<sub>4</sub> than both MTP and PhTP compounds. This behaviour can be discussed on the basis of the presence of the cyano group in the inhibitor molecule leads probably to the change of the

center of adsorption from the mercapto group (-S-H) in case of both MTP and PhTP compounds into the cyano group (-C≡N) in the case of CPhTP compound. Also, the anodic polarization curves of brass in 0.1 M H<sub>2</sub>SO<sub>4</sub> in presence of high concentrations of CPhTP compound are different than those obtained in the case of PhTP compound and there is no appearance of passivity and limiting current. This behaviour can be interpreted on the basis that CPhTP compound may be or may not formed an soluble complex Cu[CPhTP]<sup>+</sup> with Cu(I) instead of the sparingly soluble complex Cu[PhTP]<sup>+</sup> which is formed in the case of PhTP compound.

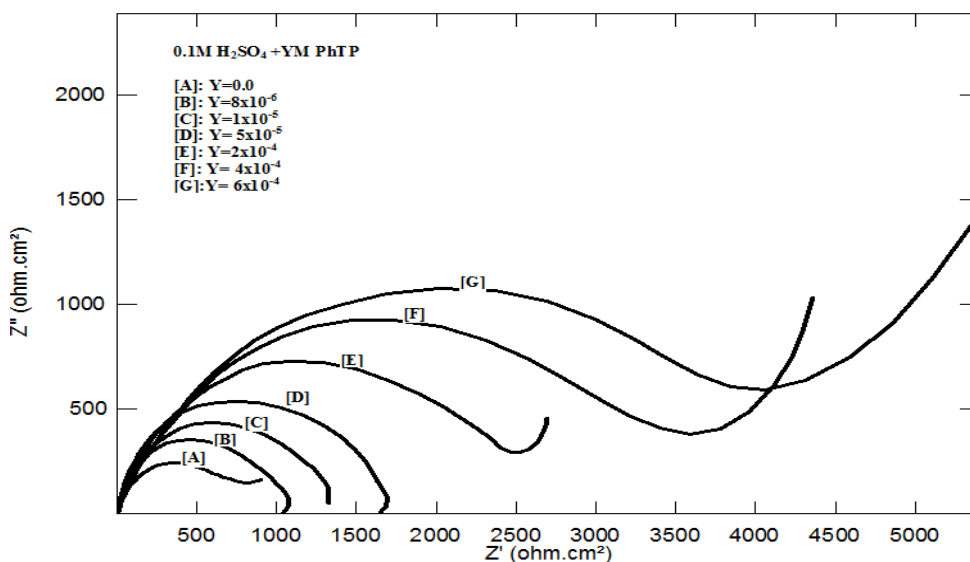
### 3.2. Electrochemical impedance spectroscopy results

Figure 6 shows the Nyquist impedance plots of brass in 0.1M H<sub>2</sub>SO<sub>4</sub> in absence and presence of different concentrations of MTP. As seen, in absence or presence of small concentrations of the inhibitor, the Nyquist impedance plot consists of distorted semicircle followed by diffusion tail indicate that the corrosion process occurs under diffusion control. The appearance of the diffusion tail in the impedance plot for copper in aerated sulfuric acid could be attributed to oxygen transport from the bulk solution to the copper surface. However, this diffusion tail disappears and replaced by capacitive loop, in presence of high concentration of the inhibitor, which could be attributed to the adsorption of MTP molecules at the metal/solution interface, this leads to the retarding of the charge transfer process of the oxidation of copper which becomes the slowest step of the corrosion reaction.



**Figure 6.** Nyquist plots of brass in 0.1M H<sub>2</sub>SO<sub>4</sub> in absence and presence of different concentrations of CPhTP

Figure 7 shows the Nyquist impedance plots of brass in 0.1M H<sub>2</sub>SO<sub>4</sub> in absence and presence of PhTP. As previously discussed for MTP, in absence of the inhibitor, the Nyquist impedance plot consists of distorted semicircle followed by diffusion tail indicate that the corrosion process occurs under diffusion control. However, this diffusion tail disappears and replaced by capacitive loop in presence of small concentrations of PhTP. This behavior can be discussed on the basis of the adsorption of PhTP molecules at the copper/solution interface as in case of the presence of high concentration of MTP. In contrary to that observed in case of MTP, at high concentration of the inhibitor, diffusion tails were obtained indicating that the corrosion reaction is controlled by diffusion of the stable complex Cu[PhTP]<sup>+</sup> from the surface of copper to the bulk solution.



**Figure 7.** Nyquist plots of brass 0.1M H<sub>2</sub>SO<sub>4</sub> in absence and presence of different concentrations of CPhTP.

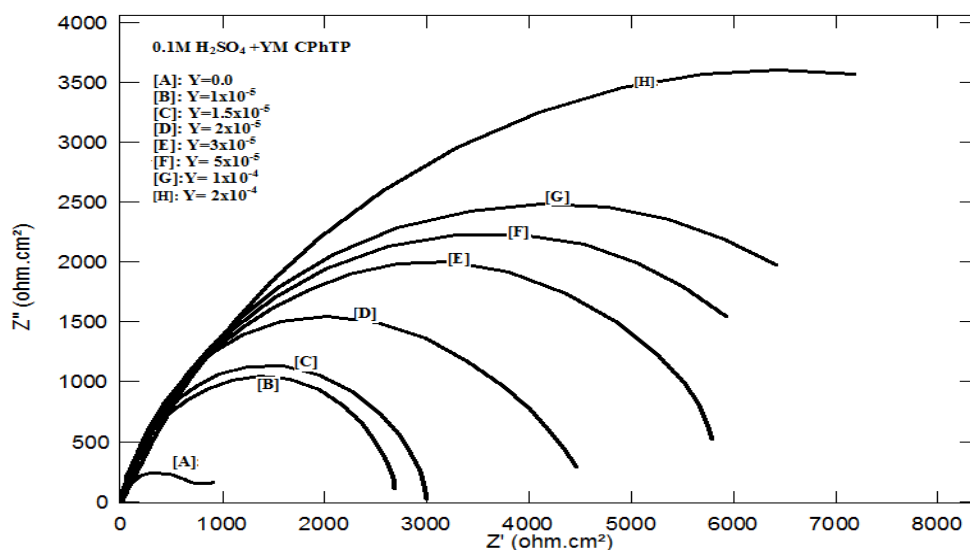


**Figure 8.** Nyquist plots of brass 0.1M H<sub>2</sub>SO<sub>4</sub> in absence and presence of different concentrations of CPhTP.

Figure 8 shows the electrochemical impedance spectroscopy plots of brass in 0.1M H<sub>2</sub>SO<sub>4</sub> in absence and presence of different concentration of CPhTP the diffusion tail disappears in presence of CPhTP, this behavior can be discussed on the basis of strong adsorption of the cyano compound, therefore the oxidation process of copper is controlled by charge transfer.

The impedance spectra of different Nyquist plots for yellow copper were analyzed by fitting the experimental data to the equivalent circuit model shown in Figure 9.

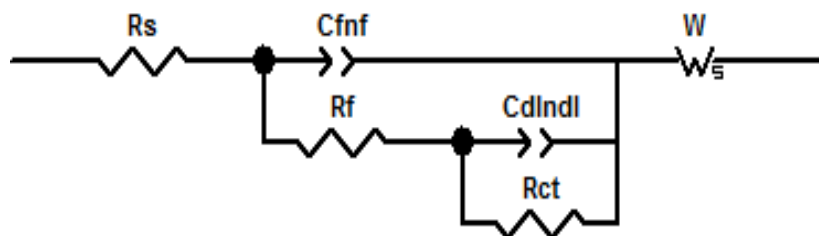


**Figure 9.** Equivalent circuit model for the corrosion of brass

The calculated parameters obtained from equivalent circuit fitting analysis with and without inhibitor in 0.1M H<sub>2</sub>SO<sub>4</sub> are given in Tables (4-6). Because of inhomogeneities in the metal surface, the capacitances were implemented as constant phase element (CPE) during analysis of the impedance plots. Two values, Q and n define the CPE. The impedance, Z, of CPE is presented by:

$$Z_{CPE} = Q^{-1} (i\omega)^{-n} \tag{6}$$

where,  $i = (-1)^{1/2}$ ,  $\omega$  is frequency in rad s<sup>-1</sup>,  $\omega = 2\pi f$  and f is the frequency in Hz. If (n) equals one, then equation 6 is identical to that of a capacitor,  $Z_C = (i\omega C)^{-1}$  where C is ideal capacitance. For non-homogeneous system, n values ranges 0.9-1 [37].

In this circuit R<sub>s</sub> represents the solution resistance between the working electrode and the reference electrode; R<sub>f</sub> is the resistance associated with the layer of products formed during immersion; R<sub>ct</sub> represents the charge-transfer resistance. Constant phase element Q<sub>1</sub> is composed of the film capacitance CPE<sub>f</sub> and the deviation parameter n<sub>1</sub>, and Q<sub>2</sub> is composed of the double-layer capacitance CPE<sub>dl</sub> and the deviation parameter n<sub>2</sub>[38]. W stands for the Warburg impedance. A Warburg diffusion tail was observed at low frequency values. A diffusion controlled process is therefore exists. Studies reported in the literature [39] showed that the diffusion process is controlled by diffusion of dissolved oxygen from the bulk solution to the electrode surface and the Warburg impedance, which is observed in the low frequency regions, is ascribed to diffusion of oxygen to the copper surface. According to the equivalent circuit, the impedance data were fitted and the electrochemical parameters were given in Tables (4-6).

The inhibition efficiency %P of different inhibitors in different concentrations is calculated by [40] :

$$\% P = [(R_{ct} - R_{ct0}) / R_{ct}] \times 100 \tag{7}$$

where R<sub>ct</sub> and R<sub>ct0</sub> represent the resistance of charge transfer in the presence and absence of inhibitors.

**Table 4.** Electrochemical impedance parameters of brass in 0.1M H<sub>2</sub>SO<sub>4</sub> in absence and presence of different concentrations of MTP

Conc, mol L <sup>-1</sup>	R <sub>s</sub> ohms.cm <sup>2</sup>	Q <sub>f</sub> x10 <sup>-5</sup> (F)	n <sub>f</sub> ohm <sup>-1</sup>	R <sub>f</sub> ohms.cm <sup>2</sup>	Q <sub>cdl</sub> x10 <sup>-5</sup> (F)	n <sub>cdl</sub> ohm <sup>-1</sup>	R <sub>ct</sub> ohms.cm <sup>2</sup>	%P
0.00	6.7	1.9	0.99	5.3	19	0.45	798	0.0
6x10 <sup>-6</sup>	6.8	4.0	0.96	7.8	5.3	0.93	1313	39.2
8 x10 <sup>-6</sup>	7.1	4.3	0.97	9.9	4.3	0.94	1570	49.1
1 x10 <sup>-5</sup>	6.9	4.2	0.98	13.5	3.5	0.94	1745	54.2
2 x10 <sup>-5</sup>	6.9	4.5	0.96	18.5	2.9	0.95	1997	60.0
5 x10 <sup>-5</sup>	6.6	3.7	0.96	12.5	3.0	0.93	2529	68.4
1 x10 <sup>-4</sup>	6.4	4.2	0.91	9.8	3.7	0.87	2675	70.1
2 x10 <sup>-4</sup>	6.6	6.4	0.85	9.6	7.6	0.61	2969	73.1
4 x10 <sup>-4</sup>	7.0	1.0	0.99	3.6	9.4	0.67	4041	80.2
6 x10 <sup>-4</sup>	6.6	2.0	0.85	203.6	11.0	0.64	4797	83.3
8 x10 <sup>-4</sup>	6.7	1.8	0.87	328.7	12.0	0.59	5183	84.6

**Table 5.** Electrochemical impedance parameters of brass in 0.1M H<sub>2</sub>SO<sub>4</sub> in absence and presence of different concentrations of PhTP

Conc, mol L <sup>-1</sup>	R <sub>s</sub> ohms.cm <sup>2</sup>	Q <sub>f</sub> x10 <sup>-5</sup> (F)	n <sub>f</sub> ohm <sup>-1</sup>	R <sub>f</sub> ohms.cm <sup>2</sup>	Q <sub>cdl</sub> x10 <sup>-5</sup> (F)	n <sub>cdl</sub> ohm <sup>-1</sup>	R <sub>ct</sub> ohms.cm <sup>2</sup>	%P
0.00	6.7	1.9	0.99	5.3	19	0.45	798	0.0
4 x10 <sup>-6</sup>	7.5	6.5	0.97	8.2	23	0.38	926	13.8
5 x10 <sup>-6</sup>	7.4	6.4	0.97	3.4	27	0.31	1066	25.1
7 x10 <sup>-6</sup>	7.6	8.1	1.08	2.1	9.9	0.82	1148	30.4
8 x10 <sup>-6</sup>	9.7	4.2	0.97	27.2	2.4	0.94	1252	36.2
1 x10 <sup>-5</sup>	10.2	4.6	0.95	23.4	2.3	0.93	1303	38.7
2 x10 <sup>-5</sup>	6.7	3.8	0.98	34.4	1.8	0.96	1464	45.4
1x10 <sup>-4</sup>	9.70	4.4	0.98	35.7	2.1	0.95	1524	47.6

The variation of percent inhibition with concentration of MTP , PhTP and CPhTP obtained from electrochemical impedance measurements for brass in 0.1 M H<sub>2</sub>SO<sub>4</sub> solution are shown in Figure 10.

The curves represent adsorption isotherms that are characterized by an initial rising part followed by leveling plateau indicating the formation of a mono-layer adsorbate film at copper surface. It is clear that the inhibition efficiency of the used inhibitors are arranged in the following order : CPhT P> PhTP > MTP . This order can be discussed on the basis that the presence of the bulky phenyl group in the PhTP molecule:(1) cover large number of the active sites of metal surface than MTP molecule and (2) increase the electron density on the adsorption center (-S-H). The highest inhibition efficiency of CPhTP is discussed above on the basis of the change of the adsorption center from the (-

S-H) group in the case of MTP and PhTP compounds into (-C≡N) group in the case of CPhTP compound.

**Table 6.** Electrochemical impedance parameters of brass in 0.1M H<sub>2</sub>SO<sub>4</sub> in absence and presence of different concentrations of CPhTP

Conc, mol L <sup>-1</sup>	R <sub>s</sub> ohms.c m <sup>2</sup>	Q <sub>f</sub> x10 <sup>-5</sup> (F)	n <sub>f</sub> ohm <sup>-1</sup>	R <sub>f</sub> ohms.cm <sup>2</sup>	Q <sub>cdl</sub> x10 <sup>-5</sup> (F)	n <sub>cdl</sub> ohm <sup>-1</sup>	R <sub>ct</sub> ohms.cm <sup>2</sup>	%P
0.00	6.7	1.9	0.99	5.3	19	0.45	798	0.0
6x10 <sup>-6</sup>	7.6	9.2	0.96	2.3	36	0.36	887	10.0
7 x10 <sup>-6</sup>	7.3	17	0.82	6.1	18	0.31	1071	25.4
8 x10 <sup>-6</sup>	7.7	10.6	0.87	7.5	20	0.37	1186	32.7
1 x10 <sup>-5</sup>	7.5	3.9	0.92	14.7	2.4	0.88	2611	69.4
1.5 x10 <sup>-5</sup>	7.3	4.2	0.87	12.4	2.9	0.84	3053	73.8
2 x10 <sup>-5</sup>	7.5	3.2	0.86	10.2	2.9	0.84	4351	81.6
3 x10 <sup>-5</sup>	7.5	1.2	0.92	6.0	0.3	0.77	5194	84.6
5 x10 <sup>-5</sup>	7.5	5.4	0.78	17.3	5.4	0.76	6785	88.2
1 x10 <sup>-4</sup>	7.3	6.4	0.74	21.8	4.3	0.81	7104	88.7
2 x10 <sup>-4</sup>	6.8	2.9	0.77	39.6	9.9	0.68	11225	92.8
4 x10 <sup>-4</sup>	7.2	1.1	0.85	62.1	7.9	0.68	13374	94.0

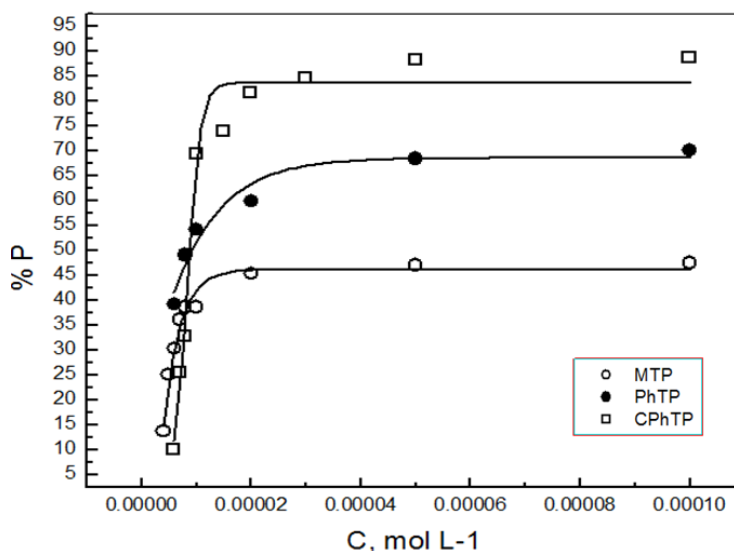


**Figure 10.** Variation of percent inhibition with the concentrations of MTP, PhTP and CPhTP for brass in 0.1 M H<sub>2</sub>SO<sub>4</sub>.

3.3. Application of the kinetic-thermodynamic model.

The action of an inhibitor in the presence of aggressive acid media, is assumed to be due to its adsorption [41] at the metal/solution interface. This phenomenon could take place via (i) electrostatic

attraction between the charged metal and the charged inhibitor molecules (ii) dipole-type interaction between unshared electron pairs in the inhibitor with the metal, (iii)  $\pi$ -interaction with the metal, and (iv) a combination of all of the above [42]. The inhibition action was regarded as simple substitutional process [43], in which an inhibitor molecule in the aqueous phase substitutes an x number of water molecules adsorbed on the metal surface, viz.



where x is the size ratio (the relative size of the inhibitor molecule to the number of surface-adsorbed water molecules) this indicates that the number of adsorbed water molecules displaced depends on the size of the adsorbate. In addition, if one is to realize that the free energy of adsorption is itself a function of surface coverage, lateral interaction effects should be included as well. The degree of surface coverage ( $\theta$ ) of the metal surface by an inhibitor was calculated using the equation:

$$\theta = (R_{ct} - R_{ct_0})/R_{ct}$$

The Kinetic-Thermodynamic model were used to fit the corrosion data of MTP, PhTP and CPhTP.

The kinetic - thermodynamic model is given by [44]

$$\log [\theta / (1 - \theta)] = \log K' + y \log C$$

where y is the number of inhibitor molecules occupying one active site. The binding constant K is given by:

$$K = K' (1/y)$$

Figures 21 shows the application of the above mentioned model to the results of adsorption of the MTP, PhTP and CPhTP on yellow copper surface. The parameters obtained from the Figures are depicted in Table 7.

The data in table 7 shows the number of active sites occupied by a single inhibitor molecules,  $1/y$ , for the three inhibitors which indicate that for the MTP compound ( $1/y= 0.70$ ) which means that the inhibitor molecule occupied one active site but in the case of PhTP compound ( $1/y=3.20$ ) it's bulky molecule occupies three active sites[44].

**Table 7.** Linear fitting parameters of MTP, PhTP and CPhTP inhibitors according to the kinetic-thermodynamic model.

inhibitor	$1/y$	K
<b>MTP</b>	0.70	79059
<b>PhTP</b>	3.20	159257
<b>CPhTP</b>	1.29	293461

However in the case of CPhTP compound ( $1/y=1.29$ ) it's molecule occupies only one active site. This result confirm the above conclusion that the presence of the cyano group in the inhibitor molecule leads to the change of the center of adsorption from the mercapto group (-S-H) to the cyano group (-C $\equiv$ N). In the case of CPhTP compound the inhibitor molecule is probably oriented



perpendicular to the surface of the copper metal rather than in line (horizontal) in the case of PhTP compound.

Since the efficiency of a given inhibitor was essentially a function of the magnitude of its binding constant  $K$ , large values of  $K$  indicate better and stronger interaction, whereas small values of  $K$  mean that the interaction between the inhibitor molecules and the metal is weaker [45]. The obtained values of  $K$  indicate that the efficiency of the inhibitors is in the same order suggested previously  $CPhTP > PhTP > MTP$ . Therefore, the inhibitive effect could be explained on the basis of the mechanism that suggests adsorption of the inhibitor molecules on the surface of the native metal acting as a film forming species decreasing the active area available for acid attack

### 3.4. Determination of the activation parameters of the corrosion reaction of brass in absence and in presence of the inhibitors.

Many industrial processes take place at high temperatures so, it is particularly important to study the variation of the inhibition efficiency with temperature. When temperature is raised, corrosive action is usually accelerated, particularly in media where evolution of hydrogen accompanies corrosion.

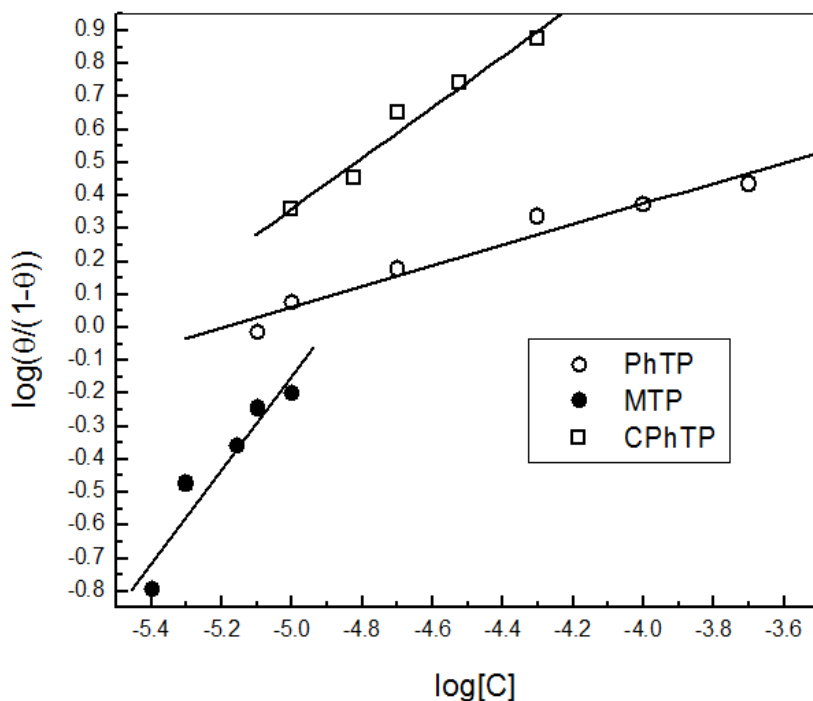


**Figure 11.** Linear fitting of the data of MTP, PhTP and CPhTP to kinetic thermodynamic model

Raising the temperature will decrease the inhibitor adsorption on the metal surface; consequently, it will lose its protective action.'

Figures (12-15) show the Nyquist plots of brass in 0.1M sulphuric acid solution, in absence and presence of MTP, PhTP and CPhTP at different temperatures.

The Nyquist impedance plot of yellow copper in 0.1M sulphuric acid in absence of inhibitors at 30°C shows a diffusion tail. This diffusion tail disappears on increasing temperature which may be attributed to increasing the oxygen diffusion from bulk solution to the metal surface. Then the charge transfer process of the oxidation of copper becomes the slow step of the corrosion reaction of copper. Similar behavior is obtained in the presence of inhibitors that might be due to changing the mechanism of corrosion. It is also observed that the size of the capacitive semicircle decreases with increasing the temperature of corrosive medium. These plots were analyzed by fitting the experimental data to the equivalent circuit that is previously used, Figure 9. The values of  $R_{ct}$  of brass in 0.1M sulphuric acid, in absence and presence of MTP, PhTP and CPhTP at different temperatures are also given in Table 8

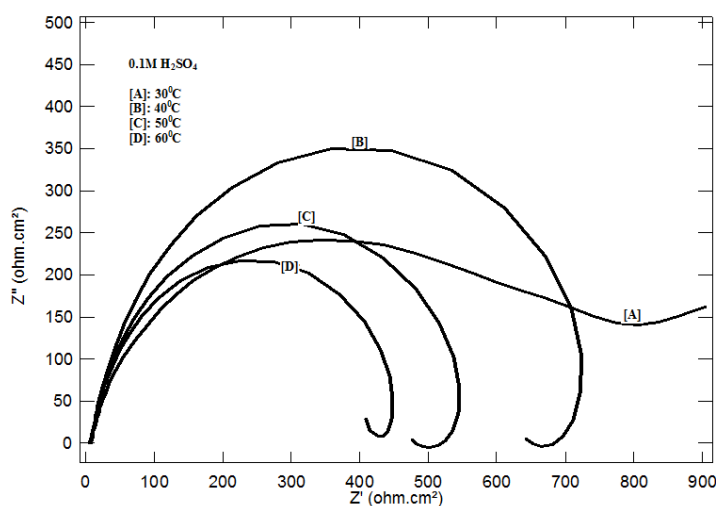


Figure 12. Nyquist plots of brass in 0.1M H<sub>2</sub>SO<sub>4</sub> solution at 30°C, 40°C, 50°C and 60°C

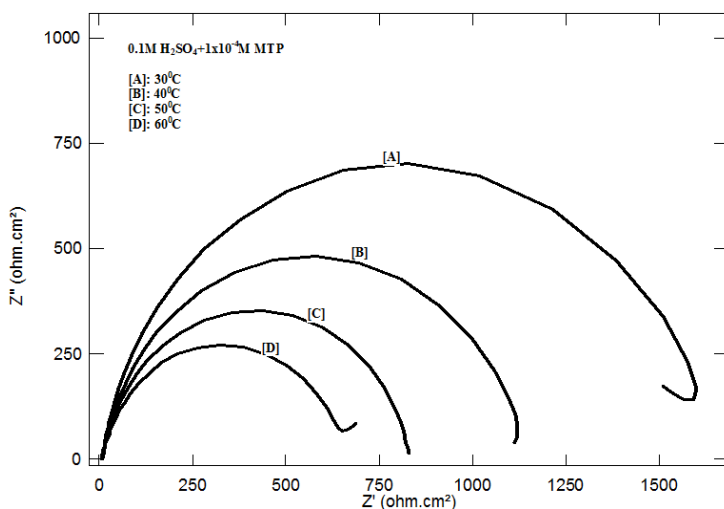
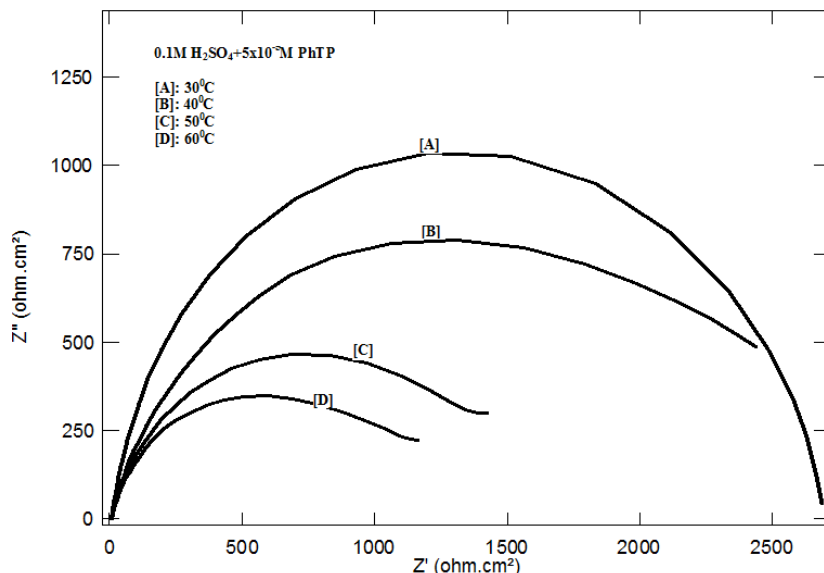
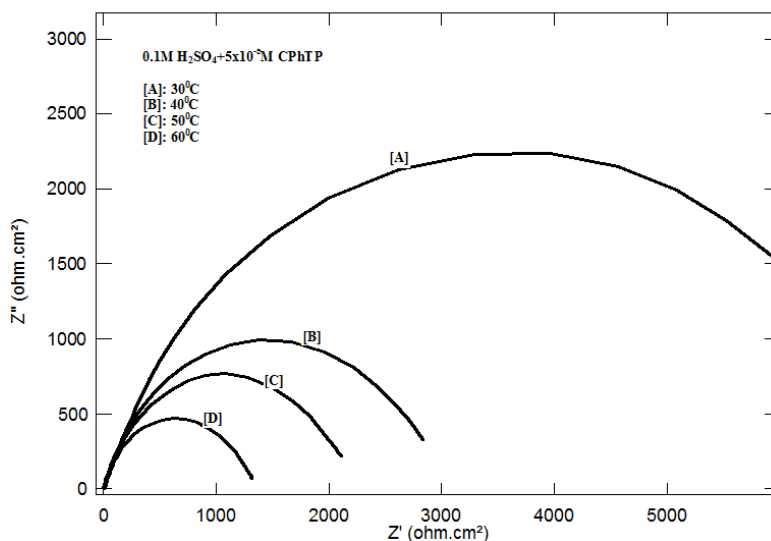


Figure 13. Nyquist plots of brass in 0.1M H<sub>2</sub>SO<sub>4</sub> in presence of 1x10<sup>-4</sup> M MTP at 30°C, 40°C, 50°C and 60°C



**Figure 14.** Nyquist plots of brass in 0.1M H<sub>2</sub>SO<sub>4</sub> in presence of 5x10<sup>-5</sup> M PhTP at 30<sup>0</sup>C, 40<sup>0</sup>C, 50<sup>0</sup>C and 60<sup>0</sup>C



**Figure 15.** Nyquist plots of brass in 0.1M H<sub>2</sub>SO<sub>4</sub>, in presence of 5x10<sup>-5</sup> M CPhTP at 30<sup>0</sup>C, 40<sup>0</sup>C, 50<sup>0</sup>C and 60<sup>0</sup>C

The tabulated data indicate that, in absence or presence of inhibitors, increasing temperature decreases the charge transfer resistance and consequently increases the corrosion rate and decreases inhibition efficiency.

In an acidic solution the corrosion rate is related to temperature by the Arrhenius equation:

$$\ln v = - Ea / RT + A$$

The corrosion rates were taken as the reciprocal of the charge transfer resistance.

It has been pointed out by many investigators [46] that the logarithm of the corrosion rate (v) is a linear function with the reciprocal of the absolute temperature 1/T where Ea is the apparent effective activation energy, T is the absolute temperature, R is the universal gas constant, and A is Arrhenius pre-exponential factor.

Enthalpy and entropy of activation  $\Delta H^*$  and  $\Delta S^*$  were obtained by applying the transition state equation. An Alternative formulation of the Arrhenius equation is the thermodynamic formulation of the transition state theory

$$v = (RT/Nh) \exp (\Delta S^*/R) \exp (- \Delta H^*/RT)$$

where, N is the Avogadro's number, h is the Plank's constant,  $\Delta H^*$  is the enthalpy of activation, and  $\Delta S^*$  is the entropy of activation. The values of  $\Delta H^*$  and  $\Delta S^*$  are calculated from the plot of  $\ln(v/T)$  versus  $1/T$ .

**Table 8.** Electrochemical impedance spectroscopy parameters of yellow copper in 0.1M H<sub>2</sub>SO<sub>4</sub> in absence and presence of MTP, PhTP and CPhTP at different temperatures

Solution	Conc, mol. L <sup>-1</sup>	Temp °C	Rs ohms.cm <sup>2</sup>	Q <sub>f</sub> x10 <sup>-5</sup> (F)	n <sub>f</sub> ohm <sup>-1</sup>	R <sub>f</sub> ohms.cm <sub>2</sub>	Qcdl x10 <sup>-5</sup> (F)	n ohm <sup>-1</sup>	Rct ohms.cm <sup>2</sup>
<b>Blank</b>	0.1M H <sub>2</sub> SO <sub>4</sub>	30	6.7	1.9	0.99	5.3	19	0.45	798
		40	7.9	4.3	0.98	28.5	2.7	0.96	673
		50	6.8	3.5	0.97	16.0	3.2	0.95	511
		60	6.7	3.9	0.98	13.3	3.5	0.95	426
<b>MTP</b>	1x10 <sup>-4</sup>	30	9.7	4.4	0.97	35.7	2.1	0.95	1524
		40	7.0	4.5	0.95	11.3	3.7	0.92	1101
		50	6.7	5.3	0.94	18.1	3.2	0.91	797
		60	6.4	4.8	0.95	12.6	5.5	0.84	647
<b>PhTP</b>	5x10 <sup>-5</sup>	30	6.6	3.7	0.96	12.5	3.0	0.93	2529
		40	6.8	7.7	0.86	22.0	11.0	0.37	2267
		50	6.4	0.5	1.10	1.9	19.0	0.78	1386
		60	6.0	9.1	0.90	121.9	46.0	0.49	1117
<b>CPhTP</b>	5x10 <sup>-5</sup>	30	7.5	5.4	0.78	17.3	5.4	0.76	6785
		40	6.9	2.2	0.91	12.5	7.6	0.76	2940
		50	6.7	6.6	0.83	22.3	2.2	0.78	1985
		60	6.4	6.6	0.84	54.1	2.1	0.81	1094

Figures 16- 18 show the plot of  $\ln v$  versus  $1/T$  and Figures 19-21 show the plot of  $\ln(v/T)$  versus  $1/T$  for the corrosion of yellow copper in 0.1M sulphuric acid solution in the absence and presence of inhibitors. The values of activation parameters were computed from the slope of the straight lines and are listed in Table 9. It is clear from the table that  $E_a$  values in the presence of the additives are higher than that in the absence. It has been stated previously[47] that, inhibitors whose percentage inhibition efficiency decrease with temperature increase, the value of activation energy ( $E_a$ ) found is greater than that in the uninhibited solution. Moreover, the value of  $E_a$  of 49.47 kJ/ mol for CPhTP indicates that the presence of cyano group in the inhibitor favour the chemical adsorption of

the inhibitor over the metal surface. On the other hand, the low values for MTP and PhTP suggest physical adsorption.

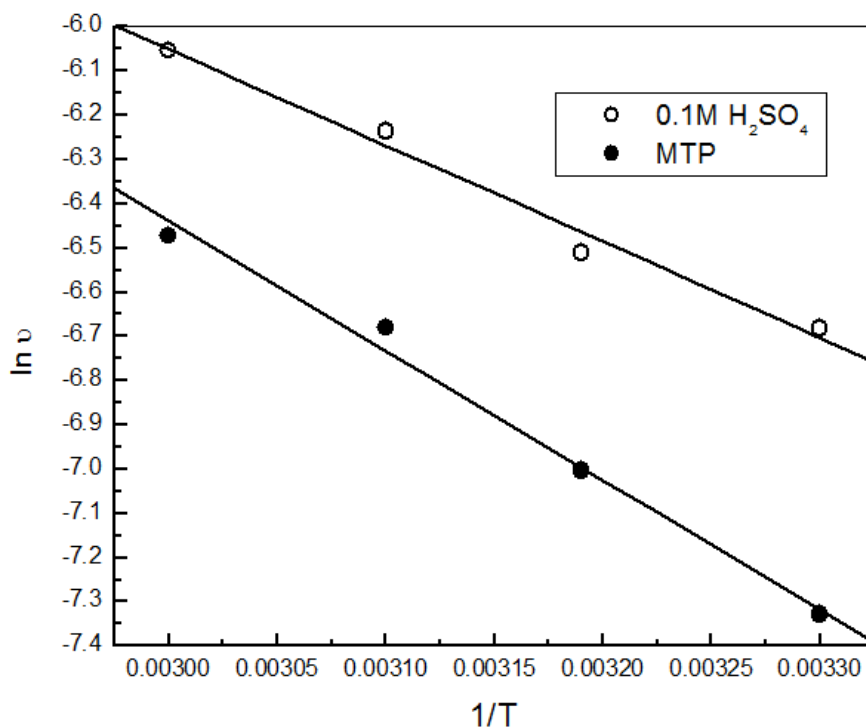


Figure 16. Linear square fit of  $\ln v$  vs.  $(1/T)$  of MTP

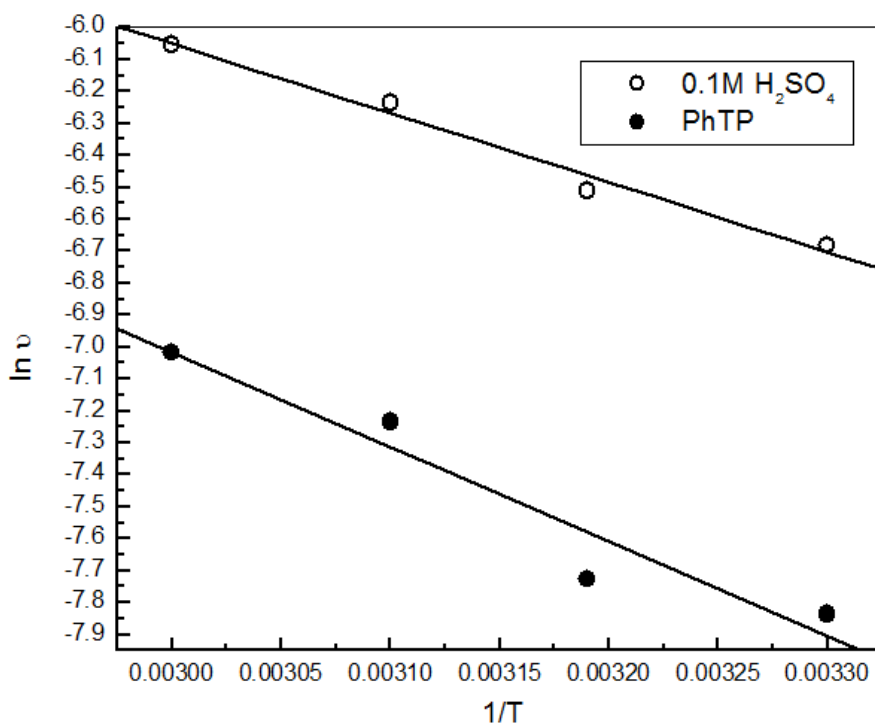
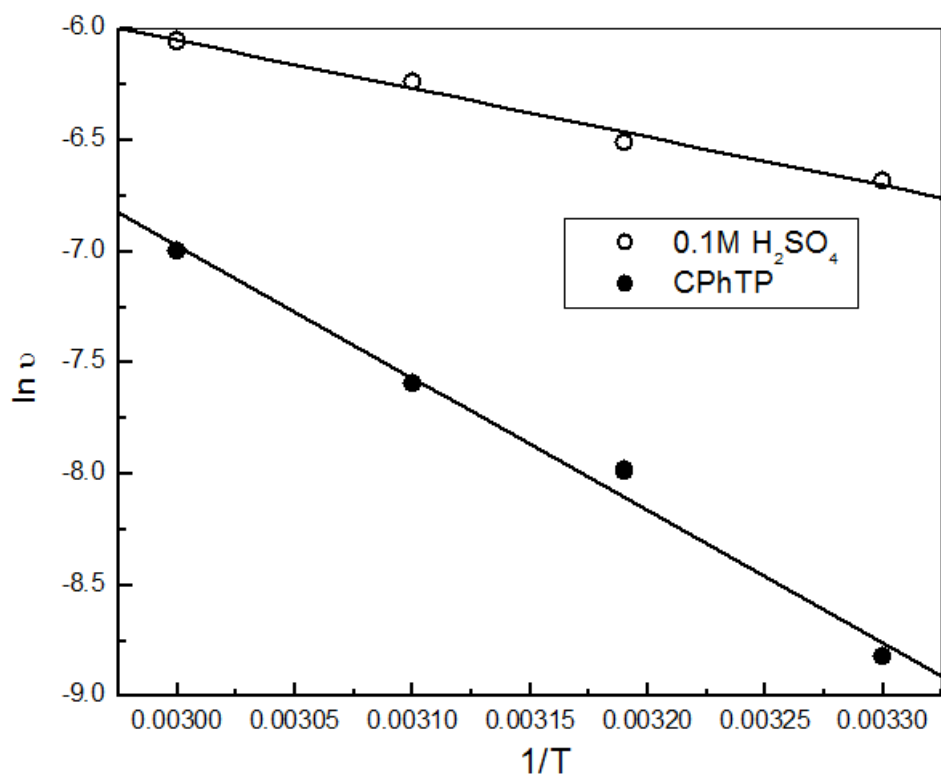
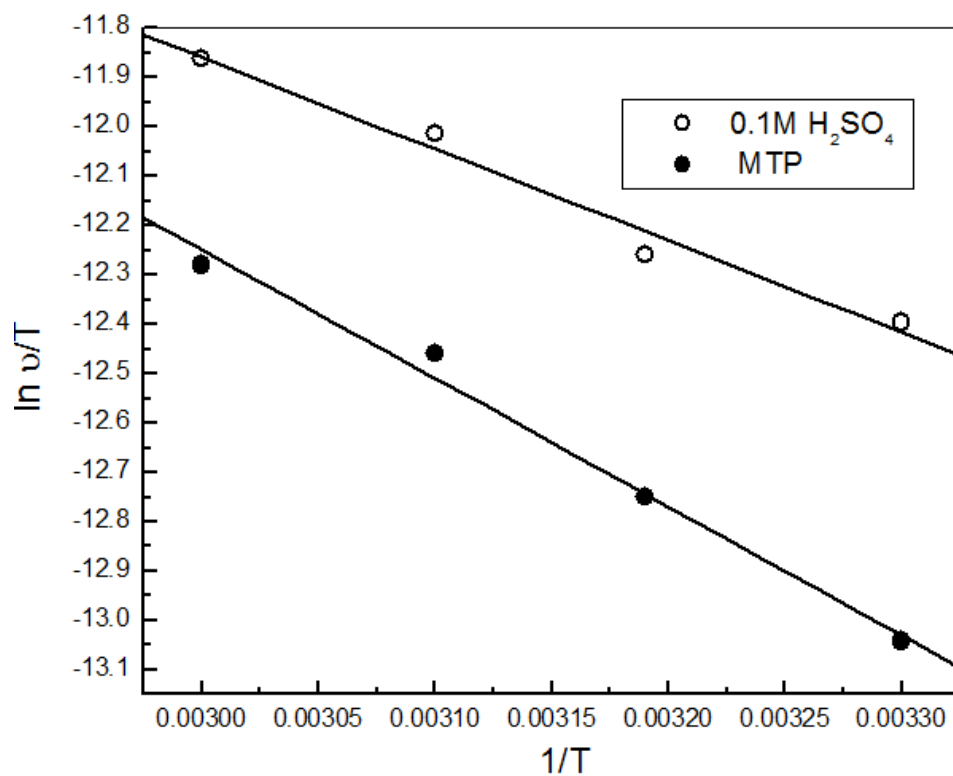


Figure 17. Linear square fit of  $\ln v$  vs.  $(1/T)$  of PhTP



**Figure 18.** Linear square fit of  $\ln v$  vs.  $(1/T)$  of CPhTP



**Figure 19.** Linear square fit of  $\ln (v/T)$  vs.  $(1/T)$  of MTP

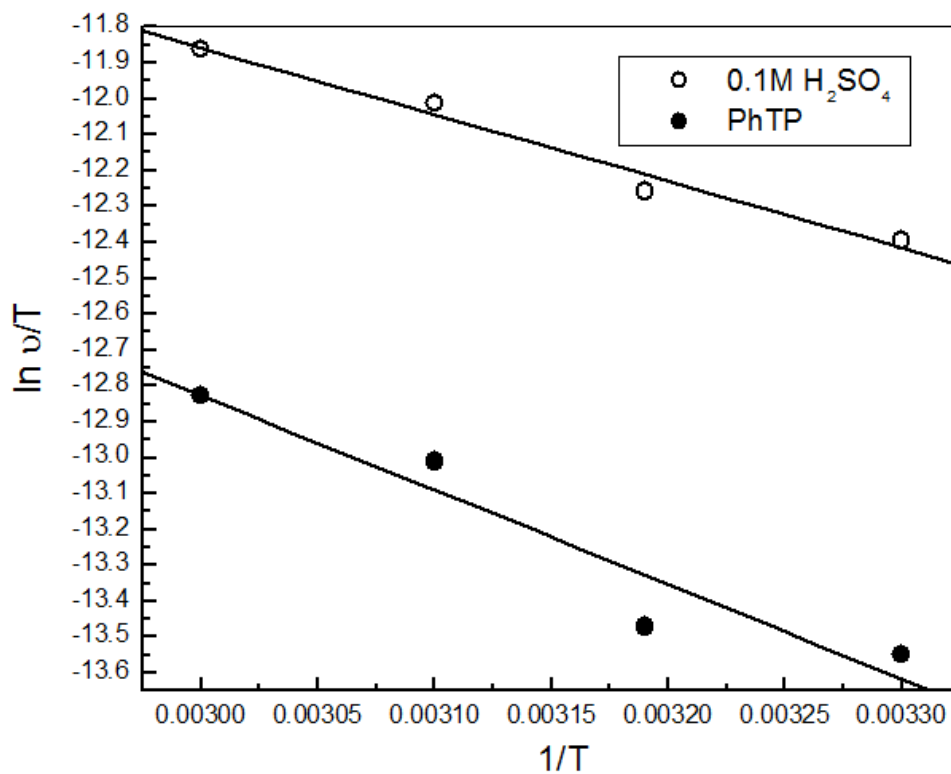


Figure 20. Linear square fit of  $\ln(v/T)$  vs.  $(1/T)$  of PhTP

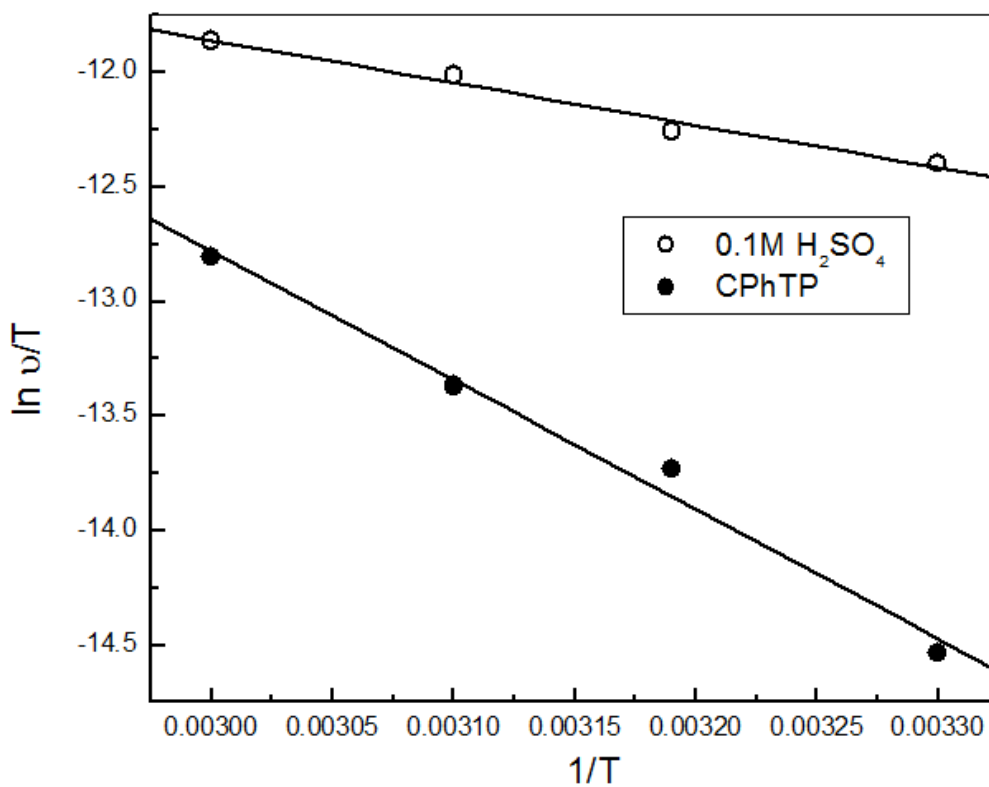


Figure 21. Linear square fit of  $\ln(v/T)$  vs.  $(1/T)$  of CPhTP

**Table 9.** The thermodynamic parameters of activation concerning brass corrosion in 0.1M sulphuric acid, in absence and presence of MTP, PhTP and CPhTP

Solution composition Conc, mol. L <sup>-1</sup>	Activation parameters		
	Ea kJ / mol.	$\Delta H^*$ kJ / mol.	$\Delta S^*$ J / mol. K
0.1M H <sub>2</sub> SO <sub>4</sub>	18.05	15.41	-249.90
0.1M H <sub>2</sub> SO <sub>4</sub> +1x10 <sup>-4</sup> M MTP	24.29	21.65	-234.42
0.1M H <sub>2</sub> SO <sub>4</sub> +5x10 <sup>-5</sup> M PhTP	24.47	21.83	-238.69
0.1M H <sub>2</sub> SO <sub>4</sub> +5x10 <sup>-5</sup> M CPhTP	49.47	46.83	-163.31

The positive values of  $\Delta H^*$  show that the adsorption of the activated complex is an endothermic process [47]. The negative value of  $\Delta S^*$  implies that the activated complex represents an association rather than a dissociation step, meaning that a decrease in disordering takes place going from reactants to the activated complex.[48,49]. The values of the activation parameters for the inhibited solution gave an indication of their dependency on the molecular structure of the inhibitor [50]. It is observed, from figure 10 that CPhTP has the highest complex structures whereas MTP has the lowest. The effect of internal motions of rotation and vibration in reactants and activated complex and the change in the number of degrees of freedom are the major contribution to the entropy of activation.

#### 4. CONCLUSIONS

- Thiopyrimidinone derivatives can be used as corrosion inhibitors for copper and its alloys in acidic media.
- Potentiodynamic polarization results have shown that MTP acts as anodic type inhibitor while both PhTP and CPhTP compounds act as mixed type inhibitors for the corrosion of brass in acidic media.
- In presence of high concentrations of PhTP the anodic polarization curves show a passivity and limiting current behavior which is due to the formation of sparingly soluble complex  $Cu[PhTP]^+$ .
- The results of the investigation show that the inhibiting properties of the three compounds depend on concentration and molecular structure of inhibitor, since comparing the results of PhTP and CPhTP indicated that the presence of cyano group in CPhTP increases the inhibition efficiency but don't form a complex.
- Electrochemical impedance spectroscopy measurements gives an indication of the change of the corrosion mechanism from adiffusion controlled to charge transfer controlled process in presence of CPhTP compound.
- Fitting the data of the three inhibitors for the corrosion of brass in 0.1 M H<sub>2</sub>SO<sub>4</sub> obeys the kinetic-thermodynamic model.



- Calculation of activation parameters shows that the presence of cyano group in CPhTP favours chemical adsorption of the inhibitor over the metal surface. On the other hand, the low values for MTP and PhTP suggest physical adsorption.

## References

1. M.M.Antonijevic, S.M. Milic and M.B. Petrovic, *Corros.Sci*, 51 (2009) 1228.
2. F.M.Kharafi , B.G.Ateya and R.M.Abd Allah, *J.Appl.Electrochem.*, 34 (2004) 47.
3. B.B.Mozeton. *corros.per.control.*, 32 (1985) 122.
4. H.C.shih and R.J.Tzon..*J.Electrochem.Soc.* , 138 (1991) 958.
5. M.I.Abbas.*Br.Corros.J.* , 26 (1991) 273.
6. G.Quartarone, G.Moretti and T.Bellomi, *Corrosion*, 54 (1998) 606.
7. F.Mansfeld , T.Smith and E.P.Parry.*Corrosion* , 27 (1971) 289
8. T.Notoya and W.Poling.*Corrosion* , 32 (1976) 216.
9. D.Chadwick and T.Hashemi. *Corros.Sci.* , 18 (1978) 39.
10. R.Ravichandran, S.Nanjundan and N.Rajndran, *J.Appl.Electrochem.*, 34 (2004) 1171
11. V.Otieno-Alego , G.A.Hope, T.Notoya and D.P.Schweinsberg. *Corros.Sci.* , 38 (1996) 213.
12. D.P.Schweinsberg, S.E.Bottle and V.Otieno-Alego. *J.Appl.Electrochem.* , 27 (1997) 161.
13. N.Huynh , S.E.Bottle , T.Notoya and D.P.Schwinsherg. *Corros.Sci.* , 42 (2000) 259.
14. G.Morretti and F.Guidi. *Corros.Sci.* , 44 (2002) 1995.
15. G.Quartarone , T.Bellomi and Zingales. *Corros.Sci.* , 45 (2003) 715.
16. D. Zhang , L. Guo and G. Zhou. *J.Appl.Electrochem.* , 35 (2005) 1081.
17. E.M.Sherif and S.Park. *Electrochim.Acta* , 51 (2006) 4665.
18. M.scendo. *Corros.Sci.* , 49 (2007) 2985 , 3953.
19. M.Scendo. *Corros.Sci.*, 50 (2008) 2070.
20. D. Zhang , L.Gayo , G.Zhou. *Corros.Sci.* , 46 (2004) 3031.
21. M. ohsawa and W.Suctaka. *Corros.Sci.* , 19 (1978) 709.
22. F.Zucchi , G. Trabaneli and C.Mnticelli. *Corros.Sci.* , 38 (1996) 147.
23. A.Davali, B.Hammouti , A.Aouniti , R.Mokhhlliss, S.Kertit and K.El Kacemi. *Aun.Chim.Sci.Mater.* , 25 (2000) 437.
24. R.Tremont , H.Dejesus-C. anada , J.Garcia-Orizco, and R.J.Costron, R.Cabrera. *J.Appl.Electrochem*, 30 (2000) 737.
25. M.Lashgari , M.R.Arshacli and M.Biglar.*J.Iran . Chem.Soc.* , 7 (2010) 478.
26. L.larali , O.Benali , S.m.Mekelleche and Y.Harek. *Appl.Surf.Sci.* , 253 (2006) 1371.
27. O.Benali , L.Larali and Harek.*J.Saudi Chem.Soc.* , 14 (2010) 231.
28. C.W.Yan , M.C.Lin and C.N.Cao.*Electrochim.Acta* , 45 (2000) 2815.
29. H.Ma, Sh.Chen, B. Yin, Sh. Zhao, X. Liu, *J.Corros. Sci.*, 45(2003)867.
30. A.H. Moreira, A.V. Benedetti, P.L. Calot, P.T.A. Sumodja., *Electrochim. Acta.*, 38 (1993)981.
31. P. Jinturkar, Y.C. Guan, K.N. Han, *Corrosion* ,54(1984)106.
32. D.K.Y. Wang, B.A.W. Coller, D.R. Macfarlane., *Electrochim. Acta.*, 38(1993)2121. E. McCafferty, *J Corros. Sci.*, 47(2005)3202.
33. R. Caban, T.W. Chapman., *J. Electrochem. Soc.*, 124(1977)1371.
34. L. L. Shreir, R. A. Jarman, G. T. Burstein, CORROSION, Vol 1, Metal/Environment Reactions, Butterworth-Heinemann, Oxford, 3<sup>rd</sup>edition (2000).
35. E.E. Foad El-Sherbini., S.M. Abdel Wahaab., M. Deyab. *Mater. Chem. and Phys.*, 89 (2005)183.
36. ZView2 help, Scribner Associates, 2000.
37. L. Hua, Sh. Zhang , W. Li, B. Hou., *J.Corros Sci.*, 52(2010) 2891.
38. H. Ma, S. Chen, L. Niu, S. Zhao, S. Li, D. Li., *J. Appl. Electrochem.*, 32(2002)65.
39. X. J. Raj and N. Rajendran., *Int. J. Electrochem. Sci.*, 6(2011)348.

40. K. Aramaki, Y. Node, and H. Nishihara., *J.Electrochem.Soc.*, 137(1990)1354.
41. D. Schweinsberg, G. George, A. Nanayakkawa, and D. Steinert., *J. Corros. Sci.*, 28(1988) 33.
42. B. Ateya, B. El-Anadouli, and F. El-Nizamy., *J. Corros. Sci.*, 24(1984)509.
43. A. El-Awady, B.A. Abd El-Nabey, and G. Aziz., *J. Electrochem. Soc.*,139 (1992) 2149
44. N. Khalil, F. Mahgoub, B.A. Abd-El-Nabey and A.. Abdel-Aziz., *CEST*, 38(2003) 205.
45. I.N. Putilova, S.A. Balezin and V.P.Barannik, *Metallic corrosion inhibitors*, Pergmon Press, Oxford, (1960).
46. E.E.Ebenso,Hailemichael Alemu, S.A Umoren and I.B.Obot.,*Int. J. Electrochem.Sci.*,3(2008)1325.
47. A.M. Abdel-Gaber, B.A. Abd-El-Nabey, I.M. Sidahmed, A.M. El-Zayady, M. Saadawy., *J. Mater Chem and Phys.*, 98(2006)291.
48. A.E. Stoyanova, E.I. Sokolova, S.N. Raicheva, *J.Corros. Sci.*, 39(1997)1595.
49. H. Ashassi-Sorkhabi and N. Ghalebsaz-Jeddi. *Mater. Chem. Phys.*, 92 (2005)480.